

Leveraging commuting groups for an efficient variational Hamiltonian ansatz

Abhinav Anand^{1,2,*} and Kenneth R. Brown^{1,2,3,4,†}

¹*Duke Quantum Center, Duke University, Durham, NC 27701, USA.*

²*Department of Electrical and Computer Engineering, Duke University, Durham, NC 27708, USA.*

³*Department of Physics, Duke University, Durham, NC 27708, USA.*

⁴*Department of Chemistry, Duke University, Durham, NC 27708, USA.*

(Dated: December 15, 2023)

Efficiently calculating the low-lying eigenvalues of Hamiltonians, written as sums of Pauli operators, is a fundamental challenge in quantum computing. While various methods have been proposed to reduce the complexity of quantum circuits for this task, there remains room for further improvement. In this article, we introduce a new circuit design using commuting groups within the Hamiltonian to further reduce the circuit complexity of Hamiltonian-based quantum circuits. Our approach involves partitioning the Pauli operators into mutually commuting clusters and finding Clifford unitaries that diagonalize each cluster. We then design an ansatz that uses these Clifford unitaries for efficient switching between the clusters, complemented by a layer of parameterized single qubit rotations for each individual cluster. By conducting numerical simulations, we demonstrate the effectiveness of our method in accurately determining the ground state energy of different quantum chemistry Hamiltonians. Our results highlight the applicability and potential of our approach for designing problem-inspired ansatz for various quantum computing applications.

I. INTRODUCTION

The last decade has seen quantum computing emerge as a transformative technology, with the potential to revolutionize various scientific fields [1–4]. A critical use of quantum computers involves simulating Hamiltonian time evolution [5] for predicting properties of different quantum systems [6]. However, the existing quantum computing platforms are in their early phases of development and encounter various sources of error, thus restricting the practical applicability of these systems [7]. This requires us to find novel algorithms that are designed to mitigate the effects of noise. One such method is to design hybrid quantum-classical algorithms [8–10] where one utilizes both the classical and quantum computer in a manner that exploits their respective strengths.

A central object of such algorithms are parameterized quantum circuits (PQCs) [11–13], which are used to prepare trial wavefunctions on the quantum computer. Recent advancements have significantly enhanced our understanding of the design principles [14, 15], trainability [16–19] and convergence properties [20] of different PQCs. A popular approach for design of PQCs are Hamiltonian based circuits [21] which are known to have better training properties [22] as they preserve the symmetry of the problem. However, these circuits often possess limitations, such as depth and subspace restrictions, which can impact their effectiveness [23, 24]. A potential solution to overcome these limitations was

proposed in Ref. [23], where the authors add driving terms to the Hamiltonian to break the problem symmetry and observe better convergence.

Another promising approach involves the utilization of Clifford or near-Clifford circuits for performing useful computation. These circuits can be simulated classically efficiently [25, 26] but are not universal, thus have a limited applications. Nevertheless, they have been used to reduce the number of measurements in quantum algorithms [27–33], find compressed representation of quantum states [34], add correlation to product wavefunctions [35] and for initial state preparation [36], among others.

In this study, we use techniques for partitioning of a Hamiltonian into commuting groups and present a novel circuit design that integrates circuits from problem-specific knowledge with general single qubit rotation gates. We employ efficient clustering techniques to construct sets of mutually commuting operators and Clifford unitaries, which simultaneously diagonalize these operator sets. Subsequently, we utilize these Clifford circuits to create "single-code" and "combined-codes" ansätze, where the Clifford circuits define a symmetric subspace of the Hamiltonian and the general rotations navigate these subspaces. We then apply these circuits to approximate ground state energies of various molecules. Finally we provide empirical evidence of better convergence of these circuit when compared to the traditional problem-based ansatz.

The remaining sections of this paper are organized as follows: Section II outlines the preliminary information and the method used in this study. Section III presents the results from numerical simulations, and finally, Section IV provides concluding remarks.

* E-mail: abhinav.anand@duke.edu

† E-mail: ken.brown@duke.edu

II. METHODOLOGY

A. Clustering Hamiltonian into commuting groups

A quantum Hamiltonian, \hat{H} , can be written as

$$\hat{H} = \sum_{k=1}^M c_k \hat{P}_k, \quad (1)$$

where c_k is a complex number and \hat{P}_k is a Pauli-string on n -qubits. A Pauli-string is defined as a tensor product of the Pauli matrices ($\hat{\sigma}_x, \hat{\sigma}_y, \hat{\sigma}_z$) and the identity operator \hat{I} as

$$\hat{P}_k = \bigotimes_{j=1}^n \hat{\sigma}_j, \quad (2)$$

with $\hat{\sigma} \in \{\hat{I}, \hat{\sigma}_x, \hat{\sigma}_y, \hat{\sigma}_z\}$. The Hamiltonian can be further separated into m -sets of mutually commuting groups as

$$\hat{H} = \sum_{k=1}^m \sum_{l=1}^{m_k} c_{kl} \hat{P}_{kl}; \quad (3)$$

$$[\hat{P}_{ki}, \hat{P}_{kj}] = 0 \quad \forall (\hat{P}_{ki}, \hat{P}_{kj}) \in \{\hat{P}_{k1}, \dots, \hat{P}_{km_k}\} \quad (4)$$

where \hat{P}_{kl} is the l -th Pauli-string in the k -th commuting set and c_{kl} is the complex coefficient. It is also well known that given a set of commuting terms, there exists a unitary, \mathcal{U} , that simultaneously diagonalizes each of the operators in the set as

$$\mathcal{U} \hat{P}_{kl} \mathcal{U}^\dagger = \bigotimes_{j=1}^n \hat{\sigma}_j, \quad \forall \hat{P}_{kl} \in \{\hat{P}_{k1}, \dots, \hat{P}_{km_k}\}, \quad (5)$$

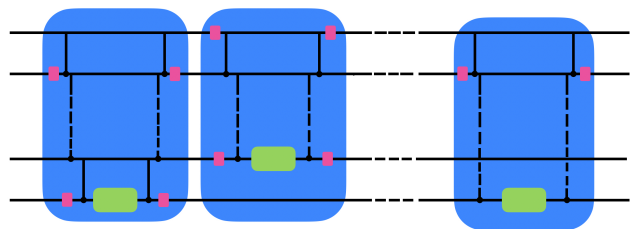
where $\hat{\sigma} \in \{\hat{I}, \hat{\sigma}_z\}$. In the past few years, several proposals [27–33] have been put forward to find the set of commuting groups, however, we follow the techniques presented in Refs. [30]. The gate complexity of the unitary, \mathcal{U} , depends on the choice of the type of commutativity, qubit wise commutativity vs. general commutativity. In this work we use the general commutativity approach, as it leads to lower number of commuting set but have deeper unitaries.

B. Variational Hamiltonian ansatz (VHA)

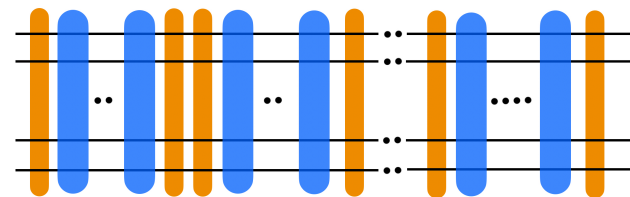
Given a Hamiltonian, \hat{H} , as in Eq. 3 we can define an ansatz as

$$U(\theta) = \prod_{k=1}^m \mathcal{U}_k \left(\prod_{l=1}^{m_k} e^{-i\theta_{kl} \hat{P}_{kl}} \right) \mathcal{U}_k^\dagger, \quad (6)$$

where $\{\theta_{kl}\}$ are variational parameters. The variational Hamiltonian ansatz is a product of unitaries that correspond to short time evolution under different parts of the Hamiltonian and can be repeated multiple times to get better approximation of the full time evolution unitary, $e^{-i\theta \hat{H}}$. A schematic representation of the VHA ansatz is shown in Fig. 1. This ansatz has been used for approximating eigenvalues of different condensed matter systems as well as for strongly correlated systems in quantum chemistry. However, they have been known to have some issues such as, limited expressibility, larger circuit depths, among others. In what follows, we present our proposed method that modifies the VHA ansatz to mitigate some of the issues.



(a) A schematic of the traditional variational Hamiltonian ansatz (VHA). A blue box represents a gate of the form $e^{-i\theta \hat{P}_i}$, where \hat{P}_i can be any Pauli-string.



(b) A schematic of the variational Hamiltonian ansatz of the form in Eq. 6. A blue box represents a gate of the form $e^{-i\theta \hat{P}_i}$, where \hat{P}_i 's are diagonal Pauli-strings.

Figure 1. A schematic of the different forms of the variational Hamiltonian ansatz. The green box represents gate of the form $e^{-i\theta \hat{\sigma}_z}$, the pink box represents gates for basis change and the orange box represents Clifford circuits (\mathcal{U}_i and \mathcal{U}_i^\dagger) for simultaneous diagonalization.

C. Modified Variational Hamiltonian Ansatz

Given a decomposition of the Hamiltonian as in Eq. 3, a set of mutually commuting terms $\{\hat{P}_{k1}, \dots, \hat{P}_{km_k}\}$ forms an abelian group. We can then construct a stabilizer group corresponding to every group by replacing some of the \hat{P}_{ki} with $-\hat{P}_{ki}$. The full procedure for constructing these stabilizer groups is as follows:

1. Collect all the terms \hat{P}_k in the Hamiltonian, $\hat{H} = \sum_{k=1}^M c_k \hat{P}_k$, which have only $\hat{\sigma}_z$ and \hat{I} in one set.

2. Use the technique in Refs. [30] to find the remaining sets and unitaries for simultaneous diagonalization. At this point we have m -sets $\{\mathcal{G}_i\}$ and m -unitaries $\{\mathcal{U}_i\}$ that diagonalize the operators within the set.
3. The stabilizer group \mathcal{S}_i corresponding to the set with only $\hat{\sigma}_z$ and \hat{I} , can be constructed by replacing \hat{P}_{ki} with $-\hat{P}_{ki}$, if there are odd number of $\hat{\sigma}_z$ acting on the first $n/2$ -qubits. A state, $|\Psi_{s_i}\rangle$, that is stabilized by this group is the Hartree-Fock state, |HF⟩ .
4. For the rest of the groups, we use their corresponding diagonal representation (which can be constructed using similarity transform with the unitaries obtained above) to replace \hat{P}_{ki} with $-\hat{P}_{ki}$ following the same procedure as for the case in step 3. A stabilizer state for these groups is the state $|\Psi_{s_i}\rangle = \mathcal{U}_i^\dagger |\text{HF}\rangle$.

The stabilizer groups $\{\mathcal{S}_i\}$ that we construct above can be considered as error-detecting codes, where the elements of the group are the stabilizers and the states $\{|\Psi_{s_i}\rangle\}$ define the codespace. We can use these stabilizer states $\{|\Psi_{s_i}\rangle\}$ and the unitaries \mathcal{U}_i to construct modified VHA ansatz. We describe the construction in detail in the following sections.

1. Single-code ansatz

We modify the unitary \mathcal{U}_i^\dagger generating the stabilizer states for each group, with a layer of general single qubit rotation to create a near-Clifford state. The resulting ansätze is of the form

$$U_{s_i}(\theta_i) = \mathcal{U}_i^\dagger \left(\bigotimes_{j=1}^n \mathbf{R}\mathbf{x}_j(\theta_{x_j}) \mathbf{R}\mathbf{y}_j(\theta_{y_j}) \mathbf{R}\mathbf{z}_j(\theta_{z_j}) \right), \quad (7)$$

where \mathcal{U}_i is the unitary that diagonalizes all the operators in the group \mathcal{G}_i , $\mathbf{R}\mathbf{x}$, $\mathbf{R}\mathbf{y}$ and $\mathbf{R}\mathbf{z}$ are single qubit rotation gates, and θ_{x_j} , θ_{y_j} and θ_{z_j} are variational parameters. We refer to these ansätze as single-code ansatz (Fig. 2) as they originate from a single abelian group.

We can use this ansatz to find the ground state of the Hamiltonian corresponding to the Hamiltonian $\hat{H}' = \sum g_i, \forall g_i \in \mathcal{G}_i$, by minimizing the following objective function

$$E(\theta) = \langle \text{HF} | U_{s_i}^\dagger(\theta) \hat{H}' U_{s_i}(\theta) | \text{HF} \rangle. \quad (8)$$

This optimization corresponds to finding the ground state of a block of the Hamiltonian, and we hypothesize that the state $U_{s_i}(\theta^*) |\text{HF}\rangle$, which is a classically simulatable state, can be a better state than the Hartree-Fock state for the full Hamiltonian. We provide empirical evidence to support this hypothesis by carrying out numerical simulations and report the result in sec. III.

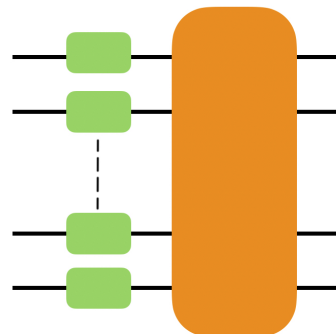


Figure 2. A schematic of a single layer of the single-code ansätze. The orange box represent Clifford circuits (\mathcal{U}_i^\dagger) and the green boxes represents a general single qubit rotation gate of the kind $e^{-i\theta_x \hat{\alpha}_x} e^{-i\theta_y \hat{\sigma}_y} e^{-i\theta_z \hat{\sigma}_z}$.

2. Combined-codes ansatz

We can then combine all the single-code ansätze to form an ansatz using the unitaries $\mathcal{U}_i \mathcal{U}_j^\dagger$ to change the basis from group \mathcal{G}_i to \mathcal{G}_j . This ansatz referred to as combined-codes ansatz (Fig. 3) can be then written as

$$U(\theta) = \prod_i^m \mathcal{U}_i^\dagger \bigotimes_{j=1}^n \mathbf{R}\mathbf{x}_j(\theta_{x_{i,j}}) \mathbf{R}\mathbf{y}_j(\theta_{y_{i,j}}) \mathbf{R}\mathbf{z}_j(\theta_{z_{i,j}}) \mathcal{U}_i, \quad (9)$$

where $\theta_{x_{i,j}}$, $\theta_{y_{i,j}}$ and $\theta_{z_{i,j}}$ are variational parameters.

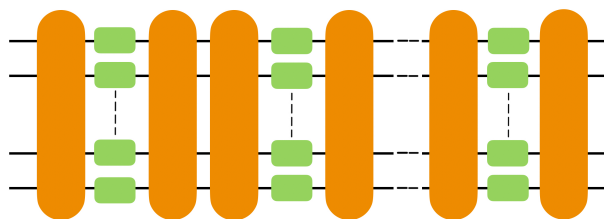


Figure 3. A schematic of a single layer of the combined-codes ansatz. The orange box represent Clifford circuits (\mathcal{U}_i and \mathcal{U}_i^\dagger) and the green boxes represents a general single qubit rotation gate of the kind $e^{-i\theta_x \hat{\alpha}_x} e^{-i\theta_y \hat{\sigma}_y} e^{-i\theta_z \hat{\sigma}_z}$.

The ordering of the different single-code ansatz is important for the full ansatz to have better convergence properties. One can use adaptive strategies [37–40] to sequentially combine these single-code ansätze to construct the full ansatz. However, that may add extra overhead in terms of circuit evaluations. So, we choose a strategy where we order them based on the 1-norm of the group.

The construction of the ansatz allows for a shorter circuit [41] with better convergence properties, as we

introduce more degrees of freedom by introducing the general single qubit unitaries within the space spanned by each commuting group. The total number of parameters in the circuit scales linearly both in the number of the qubits, n , and number of commuting groups, m .

We believe that the ansatz presented above can be used to approximate low energy eigenstates and eigenenergies within the VQE framework. We demonstrate the usefulness of the proposed ansatz by running different numerical experiments for different molecular systems and report our findings in sec. III. One can further increase the accuracy of the approximation by repeating the above ansatz multiple times.

As an illustration of our proposed framework, we provide the detailed construction of the different ansätze for the hydrogen molecule in the appendix IV.

III. NUMERICAL EXPERIMENTS

In the following we will illustrate some application of the proposed ansatz. We have implemented the whole framework using the Tequila [42] an open source package, which uses Qulacs [43] as the backend for the execution of all the numerical simulations and the BFGS implementation of SciPy [44] for gradient based optimization. We use the Jordan-Wigner transformation [45] to map the fermionic Hamiltonians of different molecules to Hamiltonians of the form in Eq. 1. The Hamiltonians used in the numerical simulations can be found here [46]. The initial values for all the circuit parameters in the different numerical simulations was fixed to 0.001.

A. Simulations with single layer

Here we present results from experiments using the single-code ansätze and a layer of the combined-codes ansatz for approximating ground state energies of different molecules using the VQE framework.

1. Small Molecules: H_2 and LiH

We first use our ansatz to approximate the ground state of the hydrogen molecule, H_2 , in the minimal basis, where we have two electrons in four spin-orbitals and the lithium hydride molecule, LiH , in an active space of the minimal basis, where we have two electrons in six spin-orbitals. The results from the simulation are presented in Fig. 4.

It can be seen from the Fig. 4, that for both the molecules H_2 and LiH , the combined-codes ansatz converges to the corresponding exact solution (FCI) in the

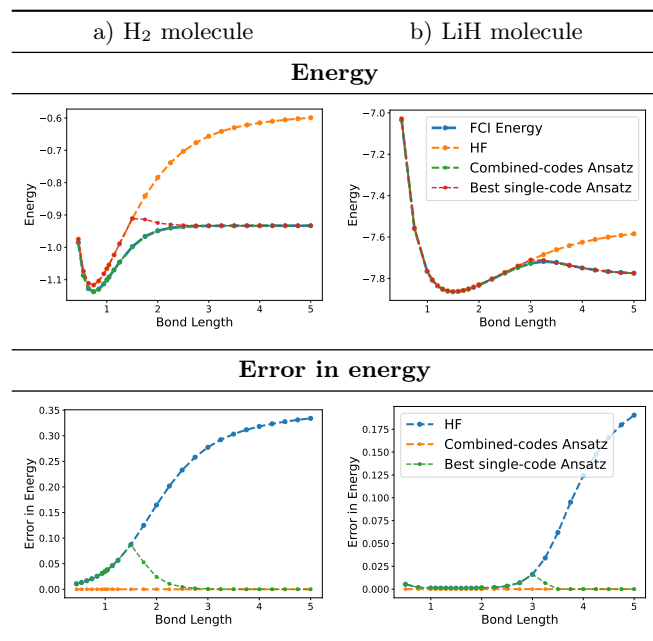


Figure 4. VQE results from optimization of ground state energies for H_2 and LiH molecule using different geometries with a single layer of the proposed ansatz.

given basis set for all geometries considered here. This implies that using a single layer of proposed ansatz is expressive enough to find good ground energy approximations for very small molecules.

Next we analyze the results from experiments using the single-code ansätze. The energy corresponding to the best single-code ansatz (the ansatz with the lowest energy) is plotted in Fig. 4. In both cases we observe that the energy corresponding this ansatz is strictly better than the Hartree-Fock (HF) energy. It converges to HF for geometries closer to equilibrium, but outperforms HF for stretched geometries.

The success of our method for approximating ground state energies of small molecules encouraged us to test our methods for larger problems.

2. Larger Molecules: H_2O and N_2

In this section, we present the results from simulations carried out for slightly larger molecules. We simulate the active space of water molecule, H_2O , which has 6 electrons in 10 spin-orbitals and an active space nitrogen molecule, N_2 , which has 6 electrons in 12 spin-orbitals. The result from all the simulations are shown in Fig. 5.

We observe that the results for these molecules using the best single-code ansatz is qualitatively similar to what we observed for the case of small molecules. It

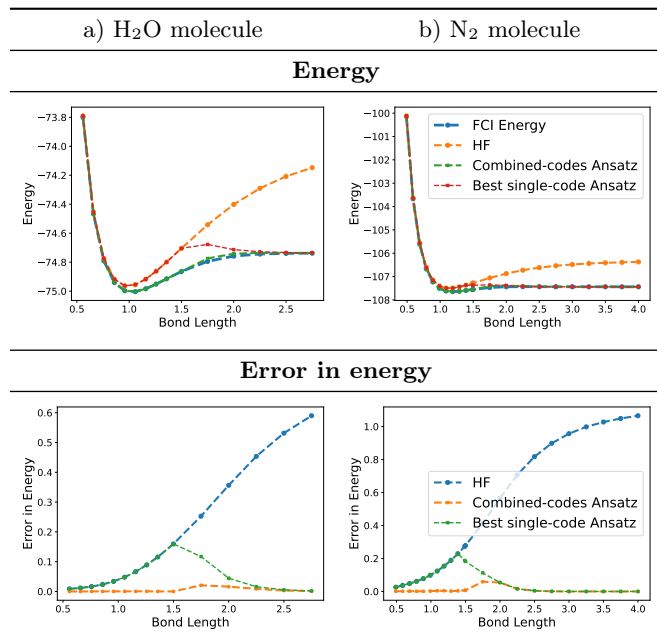


Figure 5. VQE results from optimization of ground state energies for H₂O and N₂ molecule using different geometries with a single layer of the proposed ansatz.

again converges to the HF solution for geometries near equilibrium while outperforms HF for stretched geometries. This implies that we can use the single-code ansätze for initial state preparation in regimes where the molecules have higher correlation.

Additionally, we observe that a single layer of the combined-code ansatz doesn't perform as well as for the case of the small molecules. In both cases, H₂O and N₂, the optimal energy for configurations close to the equilibrium geometry agree to chemical accuracy (1e-3) with the exact ground state energy. However, the optimal energy for stretched configurations does not converge to the exact ground state energy. We suspect that the reason behind this behavior is the limited expressivity of single layer of the proposed ansatz. This is observed in the case of the traditional VHA ansatz as well, where one needs to repeat the circuit to get better approximations. Thus, we now analyze the convergence of the proposed ansatz as a function of the number of layers used and report the results in the following section.

B. Simulation with two layers

In this section, we use the active space of the beryllium hydride molecule, BeH₂, where we have 4 electrons in 8 spin-orbitals. We run two different simulations with single and two layers of the combined-codes ansatz and show the results in Fig. 6.

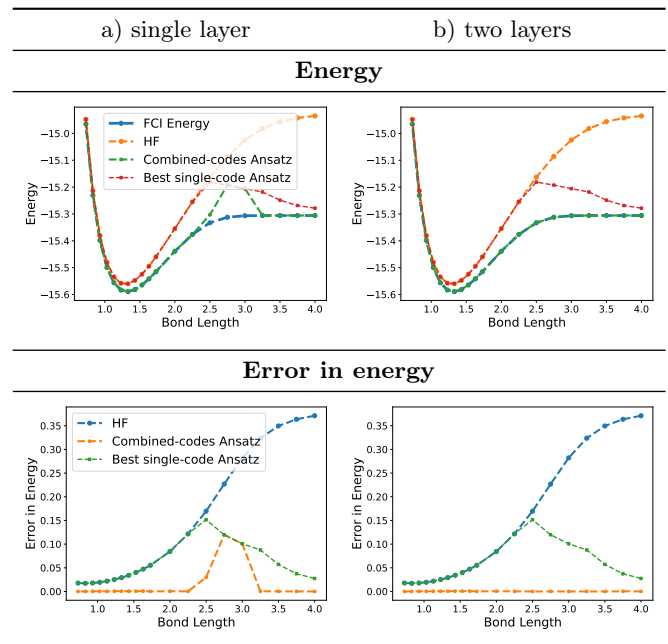


Figure 6. VQE results from optimization of ground state energies for BeH₂ molecule using different geometries with single and two layers of the proposed ansatz.

It can be seen from Fig. 6, that the energy convergence is qualitatively similar to that observed for the case of H₂O and N₂ molecules, with good convergence near equilibrium and larger errors for stretched geometries. However, the curves corresponding to the simulation with two layers of the ansatz converges to the true ground state energy for all geometries considered here. This implies that by repeating the ansatz a few times, we can get a better approximation of the eigenstates and their corresponding energies.

All the numerical experiments presented until now suggest that the ansatz proposed in this work is able to approximately find eigenvalues of molecules of varying complexity. However, we haven't provided any evidence to suggest using our method over the VHA ansatz. We provide some numerical evidence regarding that in the following section.

C. Comparison with VHA

In this section, we use the active space of the nitrogen molecule, N₂, used above in sec. III A 2, to compare the performance of the two different ansätze for three different configurations, squeezed, equilibrium and stretched.

We show the results from the different simulations in Fig. 7. It can be seen from the plots that the modified ansatz converges to a slightly better optimal energy value in comparison to the VHA ansatz, where the gap

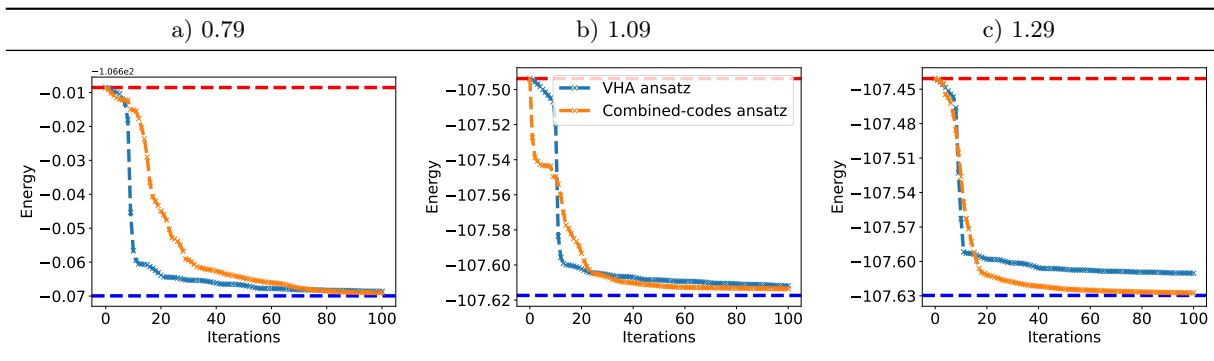


Figure 7. Optimization trajectories from simulations of the N_2 molecule with three different geometries using the traditional VHA ansatz and the proposed ansatz. The red and blue lines corresponds to Hartree-Fock and the exact ground state energies, correspondingly.

increases as we move away from equilibrium geometries towards stretched geometries. This indicates that the modified ansatz has better convergence properties for approximating eigenvalues of different molecules.

We also report the circuit complexity of the two ansätze for all the molecules considered in this work. The data is presented in Table I. We note that the modified ansatz has comparable 2-qubit gate count for the smaller molecules and significantly lower gate count for the larger molecule considered in this work, while the number of parameters are significantly higher for the modified ansatz as compared to the traditional ansatz. This suggests that we can reduce the circuit complexity of the VHA ansatz using our method for approximating eigenvalues of different molecules.

Molecule	Number of 2-qubit gates		Number of Parameters	
	VHA	M-VHA	VHA	M-VHA
H_2	36	48	14	12
LiH	262	272	61	108
BeH_2	1328	1272	184	192
H_2O	2042	1408	251	474
N_2	1860	1740	246	362

Table I. A table containing the gate complexity of a single layer of the VHA ansatz and the proposed modified ansatz (M-VHA). The values listed here are the average of all the circuits used for simulation corresponding to the different molecules.

IV. CONCLUSION

In this work, we propose a new approach for designing quantum circuits to approximate the low-lying eigenvalues of molecular Hamiltonians. We utilize efficient clustering techniques to identify groups of mutually com-

muting terms in the Hamiltonian, alongside Clifford unitaries that can simultaneously diagonalize the operators within each set. Subsequently, we introduce two distinct types of ansätze, namely the "single-code" and "combined-codes" ansatz, utilizing the stabilizer states associated with each set of commuting groups.

The proposed single-code ansatz which is classically simulatable, was shown to have better energy when compared to the widely used Hartree-Fock states for all the molecules considered in this work. These finding suggests its potential for initial state preparation for molecular geometries where HF states are not a good choice. Our work contributes to the growing research direction [34–36] of exploring practical applications of classically simulatable quantum models.

Furthermore, we provide empirical evidence confirming the utility of the combined-codes ansatz in approximating ground state energies for various molecules. Finally, we conduct a comparative analysis of the performance and gate complexity between the combined-codes ansatz and the traditional VHA ansatz. Our research marks an initial step towards the development of quantum circuits that incorporate a combination of problem-dependent and random single qubit unitaries, enabling symmetry-breaking and potentially leading to improved convergence for various problems of interest. We anticipate that the presented ansatz will unlock new possibilities for exploring the applicability of the proposed ansätze in other areas of physics and machine learning, while also providing a solid foundation for further investigations into such types of ansätze.

ACKNOWLEDGEMENTS

This work was supported by the National Science Foundation (NSF) Quantum Leap Challenge Institute of Robust Quantum Simulation (QLCI grant OMA-

2120757). A.A. also acknowledges support by the National Science Foundation (Grant No. DMS-1925919),

as part of the work was done when he was visiting the Institute for Pure and Applied Mathematics (IPAM).

-
- [1] K. Bharti, A. Cervera-Lierta, T. H. Kyaw, T. Haug, S. Alperin-Lea, A. Anand, M. Degroote, H. Heimonen, J. S. Kottmann, T. Menke, *et al.*, *Reviews of Modern Physics* **94**, 015004 (2022).
- [2] M. Cerezo, A. Arrasmith, R. Babbush, S. C. Benjamin, S. Endo, K. Fujii, J. R. McClean, K. Mitarai, X. Yuan, L. Cincio, *et al.*, *Nature Reviews Physics* , 1 (2021).
- [3] A. Anand, P. Schleich, S. Alperin-Lea, P. W. K. Jensen, S. Sim, M. Díaz-Tinoco, J. S. Kottmann, M. Degroote, A. F. Izmaylov, and A. Aspuru-Guzik, *Chemical Society Reviews* 10.1039/D1CS00932J (2022), arXiv:2109.15176.
- [4] S. McArdle, S. Endo, A. Aspuru-Guzik, S. C. Benjamin, and X. Yuan, *Reviews of Modern Physics* **92**, 015003 (2020).
- [5] R. P. Feynman, *Int. J. Theor. Phys* **21** (1982).
- [6] A. Aspuru-Guzik, A. D. Dutoi, P. J. Love, and M. Head-Gordon, *Science* **309**, 1704 (2005).
- [7] J. Preskill, *Quantum* **2**, 79 (2018).
- [8] A. Peruzzo, J. McClean, P. Shadbolt, M.-H. Yung, X.-Q. Zhou, P. J. Love, A. Aspuru-Guzik, and J. L. O’Brien, *Nature communications* **5**, 4213 (2014).
- [9] E. Farhi, J. Goldstone, and S. Gutmann, arXiv preprint arXiv:1411.4028 (2014).
- [10] J. R. McClean, J. Romero, R. Babbush, and A. Aspuru-Guzik, *New Journal of Physics* **18**, 023023 (2016).
- [11] S. Sim, P. D. Johnson, and A. Aspuru-Guzik, *Advanced Quantum Technologies* **2**, 1900070 (2019).
- [12] M. Benedetti, E. Lloyd, S. Sack, and M. Fiorentini, *Quantum Science and Technology* **4**, 043001 (2019).
- [13] I. Cong, S. Choi, and M. D. Lukin, *Nature Physics* **15**, 1273 (2019).
- [14] S.-X. Zhang, C.-Y. Hsieh, S. Zhang, and H. Yao, *Quantum Science and Technology* **7**, 045023 (2022).
- [15] Y. Du, T. Huang, S. You, M.-H. Hsieh, and D. Tao, *npj Quantum Information* **8**, 62 (2022).
- [16] J. R. McClean, S. Boixo, V. N. Smelyanskiy, R. Babbush, and H. Neven, *Nature communications* **9**, 1 (2018).
- [17] M. Cerezo, A. Sone, T. Volkoff, L. Cincio, and P. J. Coles, *Nature communications* **12**, 1 (2021).
- [18] C. O. Marrero, M. Kieferová, and N. Wiebe, *PRX Quantum* **2**, 040316 (2021).
- [19] S. Wang, E. Fontana, M. Cerezo, K. Sharma, A. Sone, L. Cincio, and P. J. Coles, *Nature communications* **12**, 1 (2021).
- [20] T. Haug and M. Kim, arXiv preprint arXiv:2104.14543 (2021).
- [21] D. Wecker, M. B. Hastings, and M. Troyer, *Physical Review A* **92**, 042303 (2015).
- [22] R. Wiersema, C. Zhou, Y. de Sereville, J. F. Carrasquilla, Y. B. Kim, and H. Yuen, *PRX Quantum* **1**, 020319 (2020).
- [23] A. Choquette, A. Di Paolo, P. K. Barkoutsos, D. Sénéchal, I. Tavernelli, and A. Blais, *Physical Review Research* **3**, 023092 (2021).
- [24] A. Anand, S. Alperin-Lea, A. Choquette, and A. Aspuru-Guzik, arXiv preprint arXiv:2209.14405 (2022).
- [25] S. Aaronson and D. Gottesman, *Physical Review A* **70**, 052328 (2004).
- [26] S. Bravyi and D. Gosset, *Physical review letters* **116**, 250501 (2016).
- [27] V. Verteletskyi, T.-C. Yen, and A. F. Izmaylov, *The Journal of chemical physics* **152** (2020).
- [28] A. F. Izmaylov, T.-C. Yen, R. A. Lang, and V. Verteletskyi, *Journal of chemical theory and computation* **16**, 190 (2019).
- [29] A. Jena, S. Genin, and M. Mosca, arXiv preprint arXiv:1907.07859 (2019).
- [30] O. Crawford, B. van Straaten, D. Wang, T. Parks, E. Campbell, and S. Brierley, *Quantum* **5**, 385 (2021).
- [31] W. J. Huggins, J. R. McClean, N. C. Rubin, Z. Jiang, N. Wiebe, K. B. Whaley, and R. Babbush, *npj Quantum Information* **7**, 23 (2021).
- [32] P. Gokhale, O. Angiuli, Y. Ding, K. Gui, T. Tomesh, M. Suchara, M. Martonosi, and F. T. Chong, *IEEE Transactions on Quantum Engineering* **1**, 1 (2020).
- [33] A. Zhao, A. Tranter, W. M. Kirby, S. F. Ung, A. Miyake, and P. J. Love, *Physical Review A* **101**, 062322 (2020).
- [34] A. Anand, J. S. Kottmann, and A. Aspuru-Guzik, arXiv preprint arXiv:2207.02961 (2022).
- [35] P. Schleich, J. Boen, L. Cincio, A. Anand, J. S. Kottmann, S. Tretiak, P. A. Dub, and A. Aspuru-Guzik, arXiv preprint arXiv:2303.01221 (2023).
- [36] G. S. Ravi, P. Gokhale, Y. Ding, W. Kirby, K. Smith, J. M. Baker, P. J. Love, H. Hoffmann, K. R. Brown, and F. T. Chong, in *Proceedings of the 28th ACM International Conference on Architectural Support for Programming Languages and Operating Systems, Volume 1* (2022) pp. 15–29.
- [37] H. L. Tang, V. Shkolnikov, G. S. Barron, H. R. Grimsley, N. J. Mayhall, E. Barnes, and S. E. Economou, *PRX Quantum* **2**, 020310 (2021).
- [38] H. R. Grimsley, S. E. Economou, E. Barnes, and N. J. Mayhall, arXiv preprint arXiv:1812.11173 (2018).
- [39] I. G. Ryabinkin, T.-C. Yen, S. N. Genin, and A. F. Izmaylov, *Journal of chemical theory and computation* **14**, 6317 (2018).
- [40] I. G. Ryabinkin, R. A. Lang, S. N. Genin, and A. F. Izmaylov, *Journal of chemical theory and computation* **16**, 1055 (2020).
- [41] E. Van Den Berg and K. Temme, *Quantum* **4**, 322 (2020).
- [42] J. S. Kottmann, S. Alperin-Lea, T. Tamayo-Mendoza, A. Cervera-Lierta, C. Lavigne, T.-C. Yen, V. Verteletskyi, P. Schleich, A. Anand, M. Degroote, *et al.*, *Quantum Science and Technology* **6**, 024009 (2021).

- [43] Y. Suzuki, Y. Kawase, Y. Masumura, Y. Hiraga, M. Nakadai, J. Chen, K. M. Nakanishi, K. Mitarai, R. Imai, S. Tamiya, T. Yamamoto, T. Yan, T. Kawakubo, Y. O. Nakagawa, Y. Ibe, Y. Zhang, H. Yamashita, H. Yoshimura, A. Hayashi, and K. Fujii, Qulacs: a fast and versatile quantum circuit simulator for research purpose (2020), arXiv:2011.13524 [quant-ph].
- [44] P. Virtanen, R. Gommers, T. E. Oliphant, M. Haberland, T. Reddy, D. Cournapeau, E. Burovski, P. Peterson, W. Weckesser, J. Bright, *et al.*, Nature methods **17**, 261 (2020).
- [45] P. Jordan and E. P. Wigner, Z. Phys. **47**, 14 (1928).
- [46] https://github.com/AbhinavUofT/Modified_VHA.

APPENDIX

In this section we present the detailed construction of the ansatz proposed in this work using the example of hydrogen molecule in the minimal basis. The Hamiltonian of H_2 in the minimal basis has 15 terms, and is:

$$\begin{aligned} \hat{H} = & -0.0984\hat{I} + 0.1713\hat{Z}(0) + 0.1713\hat{Z}(1) \\ & - 0.2230\hat{Z}(2) - 0.2230\hat{Z}(3) + 0.1686\hat{Z}(0)\hat{Z}(1) \\ & + 0.1206\hat{Z}(0)\hat{Z}(2) + 0.1659\hat{Z}(0)\hat{Z}(3) \\ & + 0.1659\hat{Z}(1)\hat{Z}(2) + 0.1206\hat{Z}(1)\hat{Z}(3) \\ & + 0.1744\hat{Z}(2)\hat{Z}(3) + 0.0453\hat{Y}(0)\hat{X}(1)\hat{X}(2)\hat{Y}(3) \\ & - 0.0453\hat{Y}(0)\hat{Y}(1)\hat{X}(2)\hat{X}(3) \\ & - 0.0453\hat{X}(0)\hat{X}(1)\hat{Y}(2)\hat{Y}(3) \\ & + 0.0453\hat{X}(0)\hat{Y}(1)\hat{Y}(2)\hat{X}(3) \end{aligned}$$

We can divide the Hamiltonian in two sets of commuting terms:

$$\begin{aligned} \mathcal{G}_1 = \{ & -0.0984\hat{I}, 0.1713\hat{Z}(0), 0.1713\hat{Z}(1), \\ & - 0.2230\hat{Z}(2), -0.2230\hat{Z}(3), 0.1686\hat{Z}(0)\hat{Z}(1), \\ & 0.1206\hat{Z}(0)\hat{Z}(2), 0.1659\hat{Z}(0)\hat{Z}(3), \\ & 0.1659\hat{Z}(1)\hat{Z}(2), \\ & 0.1206\hat{Z}(1)\hat{Z}(3), 0.1744\hat{Z}(2)\hat{Z}(3)\}, \text{ and} \end{aligned}$$

$$\begin{aligned} \mathcal{G}_2 = \{ & 0.0453\hat{Y}(0)\hat{X}(1)\hat{X}(2)\hat{Y}(3), \\ & - 0.0453\hat{Y}(0)\hat{Y}(1)\hat{X}(2)\hat{X}(3), \\ & - 0.0453\hat{X}(0)\hat{X}(1)\hat{Y}(2)\hat{Y}(3), \\ & 0.0453\hat{X}(0)\hat{Y}(1)\hat{Y}(2)\hat{X}(3)\}. \end{aligned}$$

We can then find the Clifford unitaries that diagonalizes these groups. The set \mathcal{G}_1 is already diagonal and the unitary, \mathcal{U}_{diag} , that diagonalizes the set \mathcal{G}_2 is shown in Fig. 8.

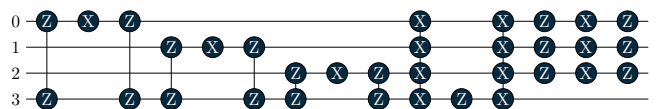


Figure 8. A Clifford unitary that diagonalizes the set \mathcal{G}_2 . The gates are represented in a compact notation, where, a gate labeled $Z(0)Z(3) == e^{-i(\pi/2)\hat{Z}(0)\hat{Z}(3)}$

The corresponding stabilizer groups can be written

as

$$\begin{aligned} \mathcal{S}_1 = \{ & \hat{I}, -\hat{Z}(0), -\hat{Z}(1), \hat{Z}(2), \hat{Z}(3), \hat{Z}(0)\hat{Z}(1), \\ & -\hat{Z}(0)\hat{Z}(2), -\hat{Z}(0)\hat{Z}(3), -\hat{Z}(1)\hat{Z}(2), \\ & -\hat{Z}(1)\hat{Z}(3), \hat{Z}(2)\hat{Z}(3)\}, \text{ and} \end{aligned}$$

$$\begin{aligned} \mathcal{S}_2 = \{ & \hat{Y}(0)\hat{X}(1)\hat{X}(2)\hat{Y}(3), -Y(0)Y(1)\hat{X}(2)\hat{X}(3), \\ & -\hat{X}(0)\hat{X}(1)\hat{Y}(2)\hat{Y}(3), \hat{X}0\hat{Y}(1)\hat{Y}2\hat{X}(3)\}. \end{aligned}$$

The corresponding stabilizer states for the two groups are:

$$\begin{aligned} |\Psi_{s_1}\rangle &= |1100\rangle \\ |\Psi_{s_2}\rangle &= \mathcal{U}_{diag}^\dagger |1100\rangle \\ &= \frac{1}{\sqrt{2}}(|1100\rangle + |0011\rangle) \end{aligned}$$

We can now use these to construct the single code ansätze for the two groups,

$$\begin{aligned} |\Psi_1(\boldsymbol{\theta}_1)\rangle &= U_{s_1}(\boldsymbol{\theta}_1) |1100\rangle \\ &= \bigotimes_{j=1}^4 \mathbf{R}\mathbf{x}_j(\theta_{x_{1,j}}) \mathbf{R}\mathbf{y}_j(\theta_{y_{1,j}}) \mathbf{R}\mathbf{z}_j(\theta_{z_{1,j}}) |1100\rangle, \text{ and} \end{aligned}$$

$$\begin{aligned} |\Psi_2(\boldsymbol{\theta}_2)\rangle &= U_{s_2}(\boldsymbol{\theta}_2) (|1100\rangle) \\ &= \mathcal{U}_{diag}^\dagger \bigotimes_{j=1}^4 \mathbf{R}\mathbf{x}_j(\theta_{x_{2,j}}) \mathbf{R}\mathbf{y}_j(\theta_{y_{2,j}}) \mathbf{R}\mathbf{z}_j(\theta_{z_{2,j}}) |1100\rangle. \end{aligned}$$

The combined codes ansatz can be then constructed as:

$$\begin{aligned} |\Psi(\boldsymbol{\theta})\rangle &= \mathcal{U}_{diag}^\dagger \bigotimes_{j=1}^4 \mathbf{R}\mathbf{x}_j(\theta_{x_{2,j}}) \mathbf{R}\mathbf{y}_j(\theta_{y_{2,j}}) \mathbf{R}\mathbf{z}_j(\theta_{z_{2,j}}) \\ &\quad \mathcal{U}_{diag} \bigotimes_{j=1}^4 \mathbf{R}\mathbf{x}_j(\theta_{x_{1,j}}) \mathbf{R}\mathbf{y}_j(\theta_{y_{1,j}}) \mathbf{R}\mathbf{z}_j(\theta_{z_{1,j}}) |1100\rangle \end{aligned}$$